Proc. Indian Acad. Sci. (Earth Planet. Sci.), Vol. 102, No. 1, March 1993, pp. 185–202.

Mean monthly wind driven climatological circulation model of the Bay of Bengal

S K DUBE, INDU JAIN, A D RAO and P C SINHA

Centre for Atmospheric Sciences, Indian Institute of Technology, Hauz Khas, New Delhi 110016, India

Abstract. A special feature of the Bay of Bengal circulation is its seasonal variation in response to the monsoonal winds. In the case of the Bay of Bengal, observationally very little is known about the large scale circulation. Theoretically, the problem of driving the circulation in the Bay of Bengal is more complex than that in other basins because of the presence of large quantities of fresh water discharge from Ganga-Brahmaputra-Meghna river systems, and also because the atmospheric driving forces even within a season are highly variable with frequent occurrences of tropical disturbances. Exploring the nature of the circulation in the Bay of Bengal is a problem of great importance in itself as well as for the critical role this region plays in the genesis of tropical disturbances which are the main source of large scale rainfall over the northern part of the Indian subcontinent. The surface circulation of the Bay of Bengal may, therefore, help in understanding the variation of rainfall over time scales ranging from the subseasonal to the interannual.

Keeping this in view, an attempt was made towards the development of an oceanic climatological circulation model for the Bay of Bengal, which explains the seasonal variability of the currents. The model is fully non-linear and vertically integrated, with realistic basin geometry. The treatment of coastal boundaries involves a procedure leading to a realistic curvilinear representation of the western and eastern sides of the Bay of Bengal. This coastal representation has the advantage of taking into account the finer resolution in the shallow regions of the northern Bay.

The model is forced by the monthly mean wind stress derived from 30 years (1950–79) of Comprehensive Oceanographic Atmospheric Data Sets (COADS). Special emphasis is given to the southern open boundary condition for the model. For this purpose, sensitivity experiments have been performed with six open boundary conditions and a comparative study of the results has been made. These sensitivity tests for the open boundary condition will help the development of a suitable coupled ocean-atmosphere model for this region. The model-generated main features are in general agreement with the known climatological circulation of the Bay of Bengal.

Keywords. Numerical model; climatological circulation; seasonal variability; Bay of Bengal; open-boundary condition.

1. Introduction

The climatic changes in the atmosphere have their counter parts in the ocean and, consequently, the changes in the conditions in the sea, reflect climatic conditions. The unique nature of the circulation in the tropical Indian Ocean, with its semi-annual reversal of winds and currents has inspired numerous models. The wind induced circulation of the North Indian Ocean has been investigated by Cox (1970) and Cane (1980). They produce the seasonal reversal of currents. But, due to coarse resolution, they are unable to simulate some features of the circulation in the Arabian Sea and the Bay of Bengal.

A number of studies have been made to simulate some features of the Arabian Sea

(Cox 1976, 1979, 1981; Hurlburt and Thompson 1976; Anderson and Moore 1979; Lin and Hurlburt 1981; Philander and Delacluse 1983; Gent *et al* 1983; Luther and O'Brien 1985; Luther *et al* 1985; McCreary and Kundu 1985, 1988; Das *et al* 1987; Simmons *et al* 1988; Dube *et al* 1990). But, the Bay of Bengal has not been studied in detail. The Bay of Bengal is the north-eastern part of the Indian Ocean. The annual reversal of monsoon winds cause a corresponding change in the flow of surface waters in the Bay (Legeckis 1987; Molinari *et al* 1990). In general, during the summer monsoon the surface waters are driven across the Bay to the eastern and north-eastern sides and these waters pile up against the coast. This accumulation results in the development of a cyclonic circulation at the head of the Bay which persists till September. To the west of the Andaman islands, the circulation is mostly anticlockwise. By way of contrast, during the winter monsoon surface waters are driven towards the south. Coupled with the lowering of surface temperatures at the head of the Bay, an anticlockwise gyre covering the entire Bay is formed during winter. It persists till April. Between these reversals, the currents are variable in both direction and strength.

Studies on the wind induced current in the Bay of Bengal are limited. But, the work of Bahulayan and Varadachari (1986); Dube *et al* (1988); Potemra *et al* (1991) and Bahulayan and Unnikrishnan (1992) is relevant. But for the study of Potemra *et al* (1991) who used the results of a multi-layer, adiabatic numerical model of the upper Indian Ocean to analyse currents in the Bay of Bengal, the other studies use vertically integrated limited area models.

A fully non-linear three dimensional model produces realistic dynamics when forced by observed wind stresses. However, they are computationally expensive. Simple vertically integrated models are useful for simulating the large scale features of the observed circulation.

Limited area models of the Bay of Bengal contain an open boundary around 6°N where the numerical domain ends, but where the fluid flow should be restricted. This is a well known problem. While Dube *et al* (1988) and Bahulayan and Vardachari (1986) used a radiation boundary condition given by Heaps (1973), the recent study of Bahulayan and Unnikrishnan (1992) tested the sensitivity of the model to two different open boundary conditions.

In our present study, we will test different open boundary conditions in order to select a suitable one for the Bay of Bengal. The model is non-linear with realistic basin geometry. It has the following features:

a) A time-dependent and vertically-integrated non-linear equation.
b) It has a free surface. In addition, the treatment of the coastal boundaries involves a procedure leading to a realistic curvilinear representation of both the western and the eastern coasts. This coastal representation has the added advantage of a finer resolution over the continental shelves.
c) Six open boundary conditions, including a clamped condition, are used to simulate the wind induced currents.
d) The computations are performed with mean monthly wind stress forcing derived from 30 years (1950–79) of Comprehensive Oceanographic and Atmospheric Data Sets (COADS). They consider the spatial variation of the wind field. As our main interest is to compute the mean monthly circulation, we use a climatological wind stress.

2. Basic equations

The formulation of the model is the same as that used by Johns *et al* (1981). This was used for the simulation of storm surges in the Bay of Bengal. In this formulation, the curvature of the earth's surface is ignored. A system of rectangular Cartesian coordinates is used in which the origin (0) is in the equilibrium level of the sea-surface. 0x points towards the east, 0y points towards the north and 0z is directed vertically upwards. The displaced position of the free surface is $z = \zeta(x, y, t)$ and the position of the sea-floor is $z = -h(x, y)$.

The basic equations of continuity and momentum are:

$$\frac{\partial u}{\partial x} + \frac{\partial v}{\partial y} + \frac{\partial w}{\partial z} = 0 \tag{1}$$

$$\frac{\partial u}{\partial t} + u\frac{\partial u}{\partial x} + v\frac{\partial u}{\partial y} + w\frac{\partial u}{\partial z} - fv = -\frac{1}{\rho}\frac{\partial p}{\partial x} + \frac{1}{\rho}\frac{\partial \tau_x}{\partial z} \tag{2}$$

$$\frac{\partial v}{\partial t} + u\frac{\partial v}{\partial x} + v\frac{\partial v}{\partial y} + w\frac{\partial v}{\partial z} + fu = -\frac{1}{\rho}\frac{\partial p}{\partial y} + \frac{1}{\rho}\frac{\partial \tau_y}{\partial z} \tag{3}$$

$$\frac{\partial w}{\partial t} + u\frac{\partial w}{\partial x} + v\frac{\partial w}{\partial y} + w\frac{\partial w}{\partial z} = -\frac{1}{\rho}\frac{\partial p}{\partial z} - g \tag{4}$$

where,

u, v, w: averaged components of velocity in the direction of x, y and z respectively;

t: time;

p: pressure;

ρ: density of the sea water assumed to be homogeneous (i.e., the thermohaline effects are neglected) and incompressible;

f: Coriolis parameter;

g: acceleration due to gravity;

τ_x, τ_y: x and y components respectively of the frictional stress (Reynolds stress).

As, thermohaline effects are more important in deep waters and our main concern is to simulate the wind induced surface circulation, these effects have been neglected.

Molecular viscosity has been neglected in these equations. The terms in τ_x and τ_y are included to model vertical turbulent diffusion. The variation of surface pressure (p_a) has negligible effect on the wind induced circulation, hence p_a is assumed constant.

Denoting the wind stress and bottom stress components as $(\tau_x^{\zeta}, \tau_y^{\zeta})$ and $(\tau_x^{-h}, \tau_y^{-h})$ respectively. The relevant boundary conditions are

$$\left.\begin{aligned} (\tau_x, \tau_y) &= (\tau_x^{\zeta}, \tau_y^{\zeta}) \\ p &= p_a \\ \frac{\partial \zeta}{\partial t} + u\frac{\partial \zeta}{\partial x} + v\frac{\partial \zeta}{\partial y} &= w \end{aligned}\right\} \text{ at } z = \zeta \tag{5}$$

$$\left.\begin{aligned} u = v = w &= 0 \\ (\tau_x, \tau_y) &= (\tau_x^{-h}, \tau_y^{-h}) \end{aligned}\right\} \text{ at } z = -h \tag{6}$$

The last condition in equation (5) is the kinematic surface condition. It expresses the fact that the free surface is materially following the fluid.

Equation (4) reduces to the hydrostatic pressure approximation

$$\frac{\partial p}{\partial z} = -\rho g \tag{7}$$

The principal equations (1), (2), (3) and (7) could be solved, but the procedure would be laborious because of the presence of a vertical coordinate. Unlike the atmosphere, a boundary layer would be needed at the top and the bottom of the domain of integration. There is insufficient knowledge about the flow in these boundary layers.

To get over this difficulty, a simplification is introduced by vertical integration. The unknown dependent variables are then, (a) the water transport (or mean current) and (b) the surface height. Integrating (1) to (3) in the vertical from $z = -h$ to $z = \zeta$ and using conditions (5) to (7), we find

$$\frac{\partial \zeta}{\partial t} + \frac{\partial}{\partial x}[(\zeta + h)\bar{u}] + \frac{\partial}{\partial y}[(\zeta + h)\bar{v}] = 0 \tag{8}$$

$$\begin{aligned}\frac{\partial \bar{u}}{\partial t} + \bar{u}\frac{\partial \bar{u}}{\partial x} + \bar{v}\frac{\partial \bar{u}}{\partial y} - f\bar{v} + \frac{1}{(\zeta + h)}\Bigg[\frac{\partial}{\partial x}\{(\zeta + h)(\overline{u^2} - \bar{u}^2)\} \\ + \frac{\partial}{\partial y}(\zeta + h)(\overline{uv} - \bar{u}\bar{v})\Bigg] \\ = -g\frac{\partial \zeta}{\partial x} + \frac{1}{(\zeta + h)\rho}(\tau_x^{\zeta} - \tau_x^{-h})\end{aligned} \tag{9}$$

$$\begin{aligned}\frac{\partial \bar{v}}{\partial t} + \bar{u}\frac{\partial \bar{v}}{\partial x} + \bar{v}\frac{\partial \bar{v}}{\partial y} + f\bar{u} + \frac{1}{(\zeta + h)}\Bigg[\frac{\partial}{\partial x}\{(\zeta + h)(\overline{uv} - \bar{u}\bar{v})\} \\ + \frac{\partial}{\partial y}\{(\zeta + h)(\overline{v^2} - \bar{v}^2)\}\Bigg] \\ = -g\frac{\partial \zeta}{\partial y} + \frac{1}{(\zeta + h)\rho}(\tau_y^{\zeta} - \tau_y^{-h})\end{aligned} \tag{10}$$

where over-bars denote the depth-averaged values, e.g.,

$$(\bar{u}, \bar{v}) = \frac{1}{(\zeta + h)}\int_{-h}^{\zeta}(u, v)\mathrm{d}z, \tag{11}$$

$$(\overline{u^2}, \overline{v^2}) = \frac{1}{(\zeta + h)}\int_{-h}^{\zeta}(u^2, v^2)\mathrm{d}z, \tag{12}$$

$$(\overline{uv}) = \frac{1}{(\zeta + h)}\int_{-h}^{\zeta} uv\,\mathrm{d}z. \tag{13}$$

In the shallow regions, particularly at the head Bay of Bengal, the non-linear terms are of special importance and must be retained in the formulation. However, the

retention in (9) of terms such as $(\overline{u^2}, \bar{u}^2)$ leads to a fundamental difficulty as they cannot be evaluated within the framework of a vertically-integrated model. In many well-documented applications of non-linear vertically-integrated equations (8) to (10), it is usual to make the assumptions

$$\begin{aligned} &\overline{u^2} - \bar{u}^2 = 0, \\ &\overline{v^2} - \bar{v}^2 = 0, \text{ and} \\ &\overline{uv} - \bar{u}\bar{v} = 0. \end{aligned} \tag{14}$$

This is equivalent to saying that the currents u and v do not vary significantly in the vertical and flow is dominated by the mid-stream flow. The validity of assumptions (14) has been demonstrated by Nihoul (1975) who has found that

$$(\bar{u}^2/\overline{u^2}) \leqslant 1{\cdot}04 \tag{15}$$

for all instants of time.

Additionally, parameterization of the bottom stress must be made in terms of the depth-averaged currents. This is frequently done by the conventional quadratic law

$$\begin{aligned} \tau_x^{-h} &= \rho c_f \bar{u}(\bar{u}^2 + \bar{v}^2)^{1/2} \\ \tau_y^{-h} &= \rho c_f \bar{v}(\bar{u}^2 + \bar{v}^2)^{1/2} \end{aligned} \tag{16}$$

where $c_f = 2{\cdot}6 \times 10^{-3}$ is an empirical bottom friction coefficient.

Substituting the values from (14) and (16) into equations (9) and (10) and expressing these equations in flux form, we get

$$\frac{\partial \zeta}{\partial t} + \frac{\partial \tilde{u}}{\partial x} + \frac{\partial \tilde{v}}{\partial y} \tag{17}$$

$$\frac{\partial \tilde{u}}{\partial t} + \frac{\partial}{\partial x}(u\tilde{u}) + \frac{\partial}{\partial y}(v\tilde{u}) - f\tilde{v} = -g(\zeta + h)\frac{\partial \zeta}{\partial x} + \frac{\tau_x^{\zeta}}{\rho} - \frac{c_f \tilde{u}}{(\zeta + h)}(u^2 + v^2)^{1/2} \tag{18}$$

$$\frac{\partial \tilde{v}}{\partial t} + \frac{\partial}{\partial x}(u\tilde{v}) + \frac{\partial}{\partial y}(v\tilde{v}) + f\tilde{u} = -g(\zeta + h)\frac{\partial \zeta}{\partial y} + \frac{\tau_y^{\zeta}}{\rho} - \frac{c_f \tilde{v}}{(\zeta + h)}(u^2 + v^2)^{1/2} \tag{19}$$

where $\tilde{u} = (\zeta + h)u$ and $\tilde{v} = (\zeta + h)v$ are new prognostic variables and $(\zeta + h)$ gives the total depth of the basin.

3. Boundary and initial conditions

In addition to the surface and bottom conditions (5) and (6), appropriate conditions have to be satisfied along the lateral boundaries for all time. Theoretically the only boundary condition needed in the vertically integrated system is that the normal transport vanishes at the coast. At the open-sea boundary, the normal current across the boundary may be prescribed.

The cross-shelf open boundaries in the present experiments are applied along the southern boundary of the analysis area (figure 1). The staggered grid of the

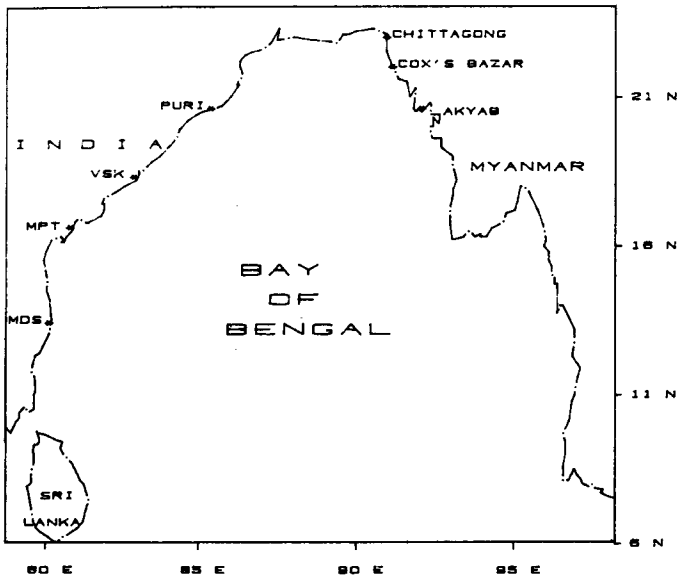

Figure 1. Analysis area of the model.

present model requires the sea-surface elevation and the velocity tangent to the open-boundary must be specified or computed at each time-step along southern open-boundary.

Six different open boundary conditions are considered which are basically the Sommerfeld radiation conditions of the form

$$\frac{\partial \phi}{\partial t} \pm c \frac{\partial \phi}{\partial x} = 0 \tag{20}$$

with a different prescription for the phase speed (or advection velocity) c, the variable ϕ represents either the sea surface elevation or the cross-shelf velocity. The upper sign in (20) is used at the southern open-boundary of the model.

The following open boundary conditions are used (Chapman 1985) in the model described by (17)–(19) to study the response of various open boundary conditions. Open boundary conditions will be hereafter denoted by "OBC" for convenience.

- *Clamped* (*CLP*): This condition assumes $c = 0$ in (20) and is the most restrictive one in the sense that boundary values do not evolve in time with the interior solution. In this case, geostrophic flow normal to the open-boundary is eliminated but both surface and bottom Ekman transport across the open-boundaries are allowed.
- *Gradient* (*GRD*): This condition assumes $c = \infty$ in (20), leading to $(\partial\phi/\partial x) = 0$. Contrary to the above condition, the boundary values in this case evolve with time and geostrophic flow normal to the boundary is allowed.
- *Gravity-wave radiation explicit* (*GWE*) *condition*: This is implemented in an explicit form. The phase speed is chosen to be the local, shallow-water surface gravity wave speed, $c = (gh)^{1/2}$.
- *Partially clamped explicit* (*PCE*) *condition*: This is similar to the gravity-wave radiation condition, but with an additional "friction like" term $(-\phi/T_f)$ on the right

hand side of (20), $T_f (= 4\,\text{hrs})$ is a friction time scale. This is also implemented in an explicit form.

- *Orlanski radiation explicit (ORE) condition*: Using the explicit form of the condition, the phase speed at which ϕ is approaching the boundary is evaluated at each time-step from values of ϕ near the boundary. The computed phase is then used in (20) at the boundary.
- *Modified Orlanski radiation explicit (MOE) condition*: This condition, suggested by Camerlengo and O'Brien (1980), uses only the extreme values of phase speed from the Orlanski radiation boundary condition ($c = 0$) or ($\Delta x/\Delta t$) computed in explicit form.

It is assumed that the motion in the sea is generated from an initial state of rest, so that

$$\zeta = \tilde{u} = \tilde{v} = 0 \text{ everywhere for } t \leqslant 0 \tag{21}$$

4. Coordinate transformation

The model covers an area lying between 6°N and 22·5°N and between 80°E and 98°E (figure 1). Western and northern coastal boundaries are situated at $x = b_1(y)$ and $y = L$ respectively. An open-sea boundary is situated at $y = 0$ corresponding to approximately 6°N. The lateral boundary at $x = b_2(y)$ corresponds to an eastern coastline. The treatment of the coastal boundaries involves a procedure leading to a realistic curvilinear representation of both the western and the eastern sides of the Bay of Bengal. This is achieved by applying a coordinate transformation

$$\xi = \frac{x - b_1(y)}{b(y)} \tag{22}$$

where $b(y) = b_2(y) - b_1(y)$ is the breadth of the Bay.

Thus, the western and the eastern boundaries correspond respectively to $\xi = 0$ and $\xi = 1$.

Taking ξ, y and t as new independent coordinates, equations (17)–(19) may be written as

$$\frac{\partial}{\partial t}(b\zeta) + \frac{\partial}{\partial \xi}\{b(\zeta + h)U\} + \frac{\partial \tilde{v}}{\partial y} = 0 \tag{23}$$

$$\frac{\partial \tilde{u}}{\partial t} + \frac{\partial}{\partial \xi}(U\tilde{u}) + \frac{\partial}{\partial y}(v\tilde{u}) - f\tilde{v} = -g(\zeta + h)\frac{\partial \zeta}{\partial \xi} + \frac{b\tau_x^\zeta}{\rho} - \frac{c_f \tilde{u}(u^2 + v^2)^{1/2}}{(\zeta + h)} \tag{24}$$

and

$$\frac{\partial \tilde{v}}{\partial t} + \frac{\partial}{\partial \xi}(U\tilde{v}) + \frac{\partial}{\partial y}(v\tilde{v}) + f\tilde{u} = -g(\zeta + h)\left[b\frac{\partial \zeta}{\partial y} - \left(\frac{\partial b_1}{\partial y} + \xi\frac{\partial b}{\partial y}\right)\frac{\partial \zeta}{\partial \xi}\right] + \frac{b\tau_y^\zeta}{\rho} - \frac{c_f \tilde{v}(u^2 + v^2)^{1/2}}{(\zeta + h)} \tag{25}$$

where,

$$U = \frac{1}{b(y)}\left[u - \left(\frac{\partial b_1}{\partial y} + \xi\frac{\partial b}{\partial y}\right)v\right] \tag{26}$$

Since all the boundaries except $y = 0$ are coastal sidewalls, the condition of zero normal velocity yields

$$u - v\frac{\partial b_1}{\partial y} = 0 \text{ at } x = b_1(y) \tag{27}$$

$$u - v\frac{\partial b_2}{\partial y} = 0 \text{ at } x = b_2(y) \tag{28}$$

and

$$v = 0 \text{ at } y = L. \tag{29}$$

At the southern boundary, we used open boundary conditions described in section 3. It may be readily shown that conditions (27) and (28) are equivalent to

$$U = 0 \text{ at } \xi = 0 \text{ and } \xi = 1. \tag{30}$$

The numerical procedure will be to solve the governing equations (23)–(25) in a rectangular computational area given by $0 \leqslant \xi \leqslant 1$, $0 \leqslant y \leqslant L$. Hence, on satisfying (30) the no flux boundary conditions at the lateral coast-lines are automatically fulfilled.

5. Numerical procedure

The discrete coordinate points in the $\xi - y$ plane are defined by

$$\begin{aligned} &\xi = \xi_i = (i-1)\Delta\xi, i = 1, 2, \ldots, m; \ \Delta\xi = 1/(m-1) \\ &y = y_j = (j-1)\Delta y, j = 1, 2, \ldots, n; \ \Delta y = L/(n-1) \end{aligned} \tag{31}$$

where, m and n are chosen to be odd and even integers respectively. A sequence of time-instants is defined by

$$t = t_p = p\Delta t, p = 0, 1, \ldots \tag{32}$$

As the model is non-linear, it requires the predictive variables to be specified at each and every grid point. Hence, the first and the simplest choice appears to be the unstaggered grid. However, the unstaggered grid cannot handle the high frequency waves, particularly the two grid waves. It is thought that the error developed at each grid point due to truncation or rounding off may give rise to two-grid oscillations due to coupling between errors at adjacent points. Calculations show that the use of a staggered grid does not produce two-grid waves, so a staggered grid has been used in which there are three distinct types of computational points. A suitable arrangement of grid points in the (ξ, y) plane is indicated in figure 2. The grid lines are all parallel to the coordinate axes and form a uniform network with a rectangular mesh having sides of length $\Delta\xi$ in the ξ-direction and Δy in the y-direction. When i is even and j

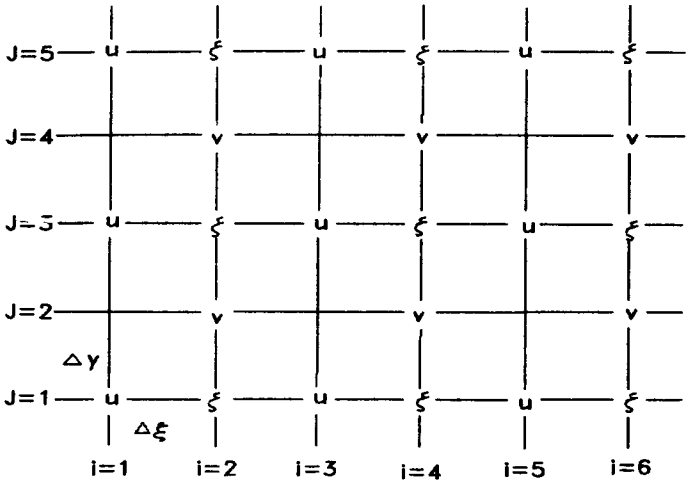

Figure 2. Grid-point arrangement.

odd, the point is a ζ-point at which ζ is computed. If i is odd and j is odd, the point is a u-point at which both u and U are computed and finally if i is even and j is even, the point is v-point at which v is computed.

The rectangular grid system is chosen to cover the whole of the Bay of Bengal. The lateral boundaries of the finite-difference grid are chosen so that the open-sea boundary (southern boundary) consists of ζ-points and u-points.

Equations (23)–(25) are then discretized and written in finite difference form for their numerical solution. The details of discretization has been described by Johns *et al* (1981). The computational stability is ensured subject only to the time-step being limited by the space increment and gravity wave speed (CFL criterian).

6. Numerical experiments

Values of m and n are taken as 51 and 50 respectively. The north-south extent, L, of the area is about 1800 km and $\Delta y = 36{\cdot}5$ km. The east-west space increment varies between 35 km at 6°N and 9 km at 22°N.

The idealised bathymetry has a depth of about 10 m near the coast and a maximum depth of about 500 m at the central part of the Bay of Bengal. In reality, the maximum depth of water is greater than that used in the model. But, from the point of view of wind induced circulation, 500 m is deep enough and an increase in the depth has little effect on the wind induced currents. The model is forced by the climatological monthly mean winds. We use thirty-year average (1950–79) winds on a 2° × 2° grid. A bicubic spline is then used to interpolate the wind from their 2° resolution down to the model resolution. The wind stress is computed by using a bulk-aerodynamic formula

$$\tau = \rho_a C_D |\mathbf{V}_a| \mathbf{V}_a$$

where τ is the wind stress vector, ρ_a is the density of the air, C_D is a drag coefficient and $\mathbf{V}_a$ is the wind vector. Values of ρ_a and C_D are $1{\cdot}176\,\mathrm{kg\,m^{-3}}$ and $1{\cdot}25 \times 10^{-3}$.

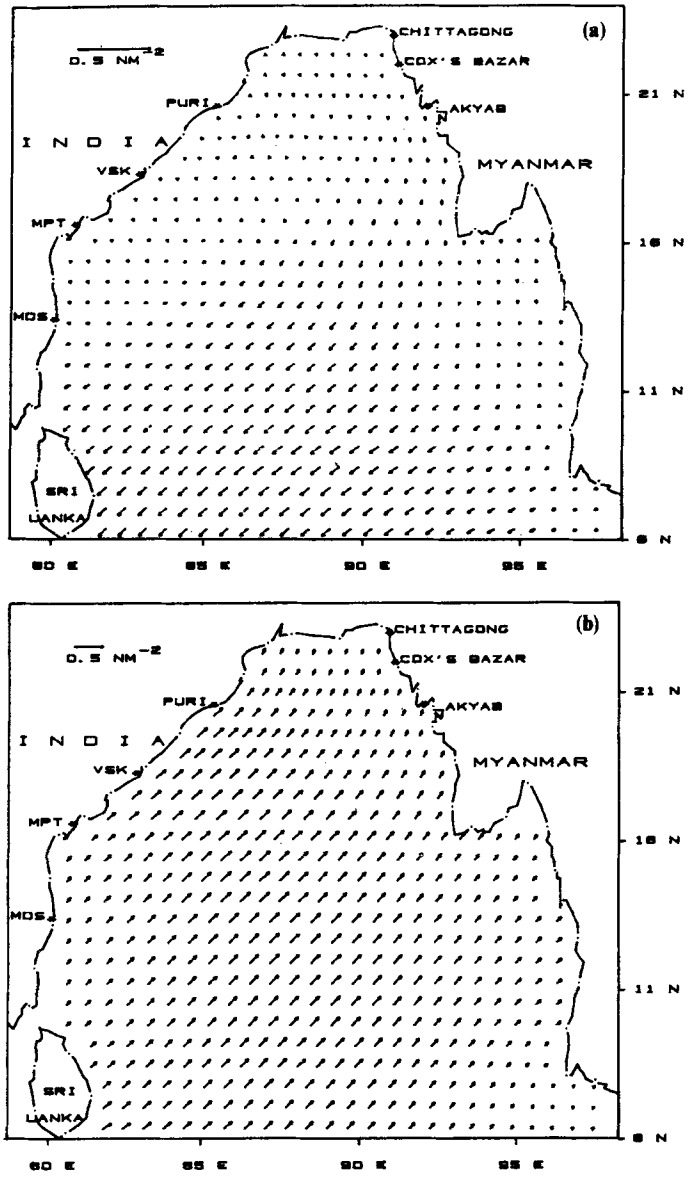

Figure 3. Mean monthly wind stress (a) February (b) July. The units are Newton per m^2.

Figure 3a and 3b depict the mean wind stress of February and July. These are representative months for the winter and summer monsoons. In the Bay of Bengal the winds are northeasterly during the winter months (figure 3a) and they change to southwesterly winds during summer months (figure 3b). This seasonal reversal during the year causes the reversal of currents. A comparison of the wind stresses reveal that for July it is about 2·8 times stronger than in the month of February. To maintain computational stability, the time step (Δt) is taken as 3 min. In the numerical experiments an initial state of rest is prescribed and the governing equations are

integrated ahead in time. Ten to twelve days of integration of the model leads to a steady state circulation over the Bay of Bengal.

A number of sensitivity experiments are performed by applying different conditions at the southern boundary. We wish to examine the effect of these conditions on the wind induced circulation of the Bay of Bengal. The currents have been computed for all the twelve months, but the results are presented only for February and July.

7. Results and discussion

We will first examine the model produced wind driven circulation during the summer monsoon (July). After integrating the model to a steady state, which is achieved in 12 to 14 days, a comparison of the results with different boundary conditions will be made.

7.1 *Summer monsoon*

The circulation in the Bay of Bengal during the summer is a complicated system of cyclonic and anticyclonic eddies of the order of 100 to 1000 km (Düing 1970). However, at some time in summer, the flow in the Bay of Bengal may be described as being generally cyclonic throughout. Some of the main features of the circulation during July are: (a) a weak anticyclonic outdraft off the Madras coast, (b) the currents along the east coast of India do not completely follow the coast line and they have an eastward tendency, (c) a large eastward transport of water off Visakhapatnam around 15°N and, (d) a cyclonic circulation in the head Bay. These features are shown in figure 4 (La Violette 1967).

Figures 5 (a, b, c, d, e, f) depict the model's computed circulation corresponding to CLP, GRD, GWE, PCE, ORE and MOE open-boundary conditions. These figures correspond to the circulation generated after 14-days of integration. While a steady state was achieved for CLP, GWE, ORE and MOE in about 12-days, the application of GRD and PCE do not produce a steady state circulation even after 30-days of

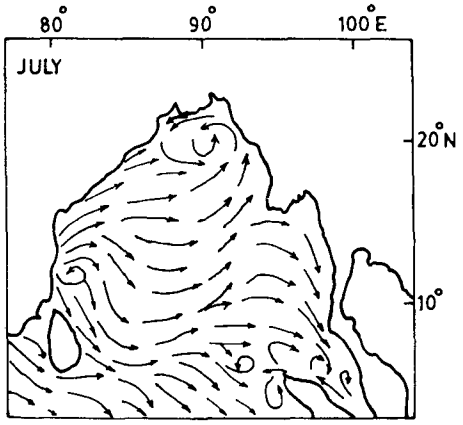

Figure 4. Large scale climatological circulation as observed during the month of July (La Viollette 1967).

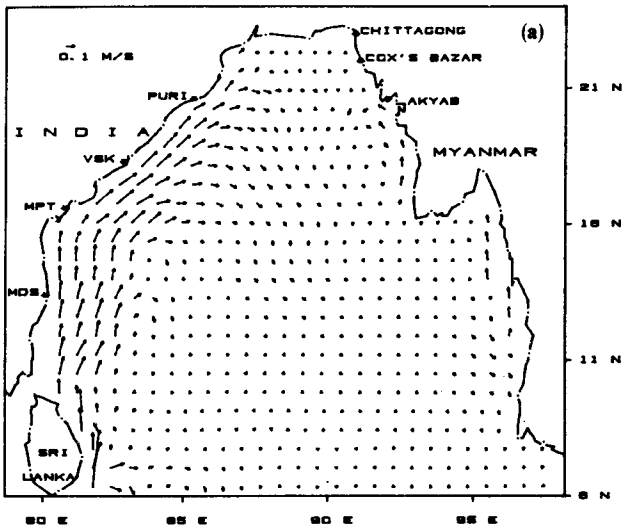
(a)
0.1 M/S
CHITTAGONG
COX'S BAZAR
AKYAB
PURI
INDIA
VSK
MYANMAR
MPT
MDS
SRI
LANKA
21 N
16 N
11 N
6 N
80 E
85 E
90 E
95 E

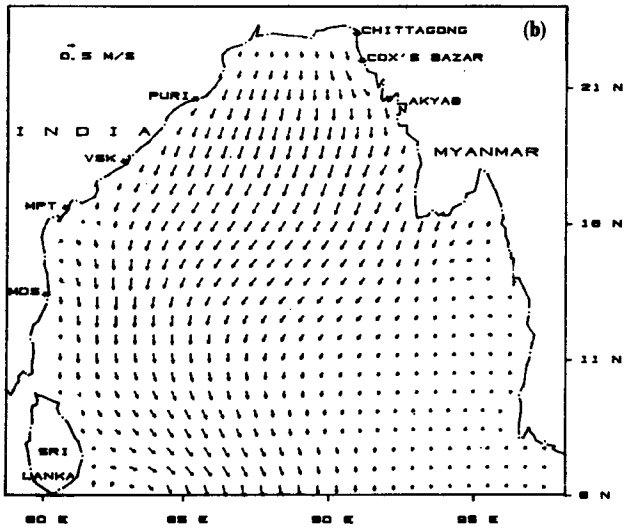
(b)
0.5 M/S
CHITTAGONG
COX'S BAZAR
AKYAB
PURI
INDIA
VSK
MYANMAR
MPT
MDS
SRI
LANKA
21 N
16 N
11 N
6 N
80 E
85 E
90 E
95 E

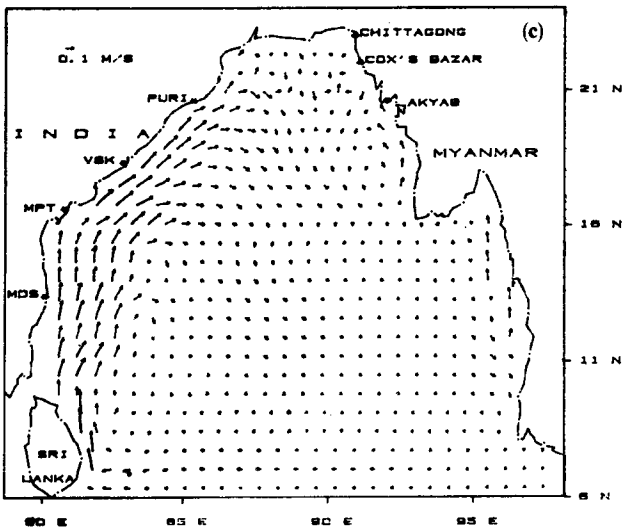
(c)
0.1 M/S
CHITTAGONG
COX'S BAZAR
AKYAB
PURI
INDIA
VSK
MYANMAR
MPT
MDS
SRI
LANKA
21 N
16 N
11 N
6 N
80 E
85 E
90 E
95 E

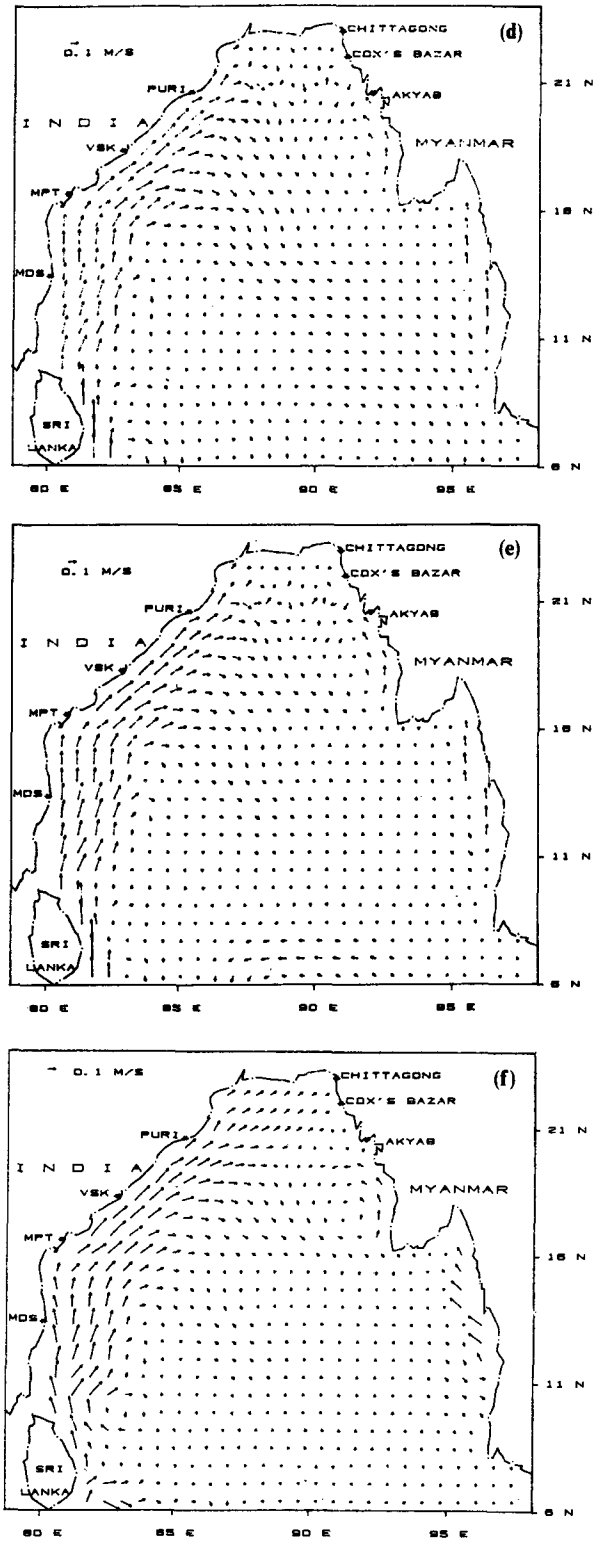

Figure 5. Simulated circulation pattern for the month of July with (a) CLP (b) GRD (c) GWE (d) PCE (e) ORE (f) MOE.

integration. The results get rapidly contaminated with very high values of currents and sea surface elevation in the whole region.

A comparison of the simulated circulation produced by using CLP (figure 5a) with the climatological circulation (figure 4) shows that the model is not able to produce many general circulation features realistically. In the head Bay, the circulation does not give a realistic pattern. Anticyclonic eddies off the Madras coast are also not produced very well. The flow pattern corresponding to GWE condition (figure 5c) is worse when compared with the previous simulation. An unrealistically strong eastward flow develops in the vicinity of the southern open boundary (6°–7°N). The circulation produced by ORE (figure 5e) is almost identical to that of the earlier result (figure 5c) with minor differences.

The experiment with MOE gives a reasonably satisfactory circulation pattern (figure 5f). We find from the figure that a weak anticyclonic outdraft is simulated around 12°N off the east coast of India. Strong currents along the east coast of India having a large eastward transport of water off the Visakhapatnam coast ($\sim$ 16°–17°N) is in agreement with the climatological circulation. The model also simulates a cyclonic eddy in the northeastern region of the Bay of Bengal with its centre around 93°E, 17°N. The simulated cyclonic circulation in the head Bay is slightly to southeastward of its observed location. This may be because the model has simulated only wind induced currents; it does not take into account other factors which may determine the circulation in this region. The head Bay is joined by one of the world's major river system, namely, the Ganga-Brahmaputra-Meghna. The large fresh water discharge from these rivers during the summer monsoon period may modify the circulation (Somayajulu *et al* 1987).

Figure 6 shows the contours of sea-surface elevation computed with the model for July. As this model is barotropic, divergence or convergence will appear in the form of sea-surface elevations. In the present work, positive sea-surface elevations are

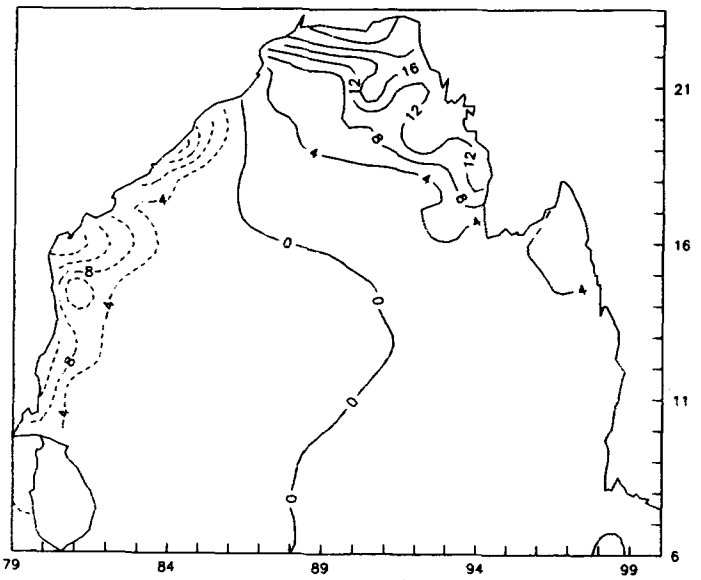

Figure 6. Contours of the sea surface elevation for the month of July (cm). Dashed lines indicate negative values (upwelling) and solid lines represent positive values (downwelling).

interpreted as convergence (downwelling) and negative elevations as divergence (upwelling). The areas of computed negative sea-surface elevations along the east coast of India are in good agreement with the observed upwelling along the coast. The negative sea-surface elevations all along the east coast of India extending upto 20°N may be attributed to offshore surface Ekman transport associated with a dominant eastward component of the western boundary current. The model computed positive sea-surface elevations in the head Bay are the result of entrainment of water towards the northeast region. This is in good agreement with the inferences of Rao (1977).

7.2 *Northeast monsoon*

In this section we will discuss the wind driven circulation during winter (February). The results obtained by applying MOE will be presented as only this open boundary condition produces a realistic circulation in the Bay of Bengal.

The circulation in the Bay of Bengal (north of 10°N) during the northern winter is anticyclonic. The western part of the circulation forms an intense western boundary current flowing northward along the east coast of India (Legeckis 1987). South of 10°N the currents in the Bay of Bengal are generally westwards. Figure 7 shows the large scale circulation pattern during February compiled by La Violette (1967).

Figure 8 shows the model computed circulation during February. The circulation reveals a large anticyclonic gyre centered at 16°N, 85°E. This is consistent with the climatological circulation (figure 7). The western end of this gyre consists of relatively strong and narrow currents flowing northwards along the east coast of India. The presence of this western boundary current has been illustrated by Legeckis (1987) with the help of satellite SST imageries. The model is also able to produce a general westward flow south of 10°N as a part of the North Equatorial Current which prevails during this period of the year.

The sea-surface elevations computed for February are shown in figure 9. We find that sea-surface elevations are positive along the east coast of India south of 17°N. Weak negative elevations (upwelling) are seen along the Orissa coast which are attributed to the presence of the western boundary current. Strong negative values

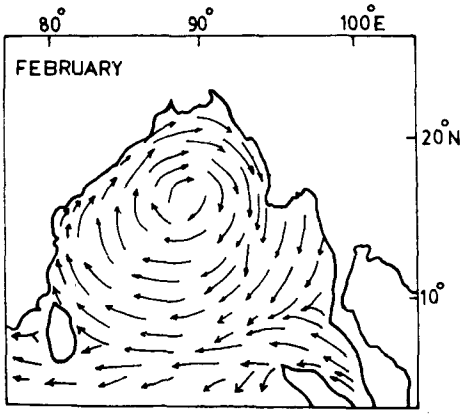

Figure 7. Large scale climatological circulation as observed during the month of February (La Viollette 1967).

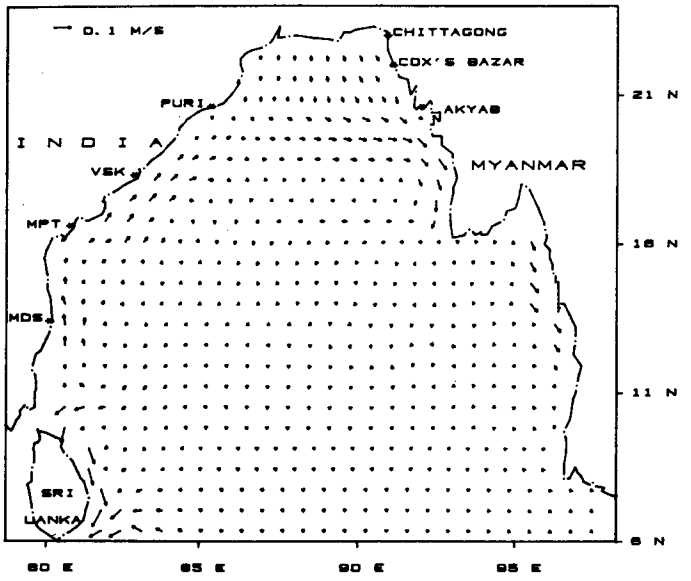

Figure 8. Simulated circulation pattern for the month of February with MOE.

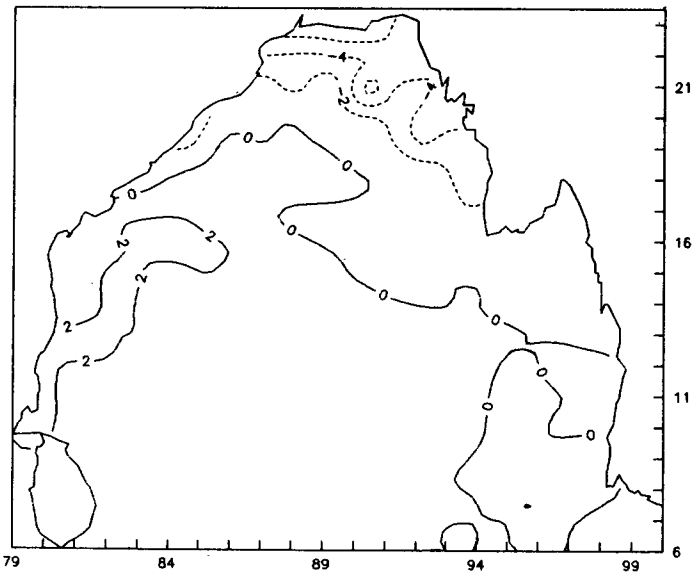

Figure 9. As in figure 6 except for the month of February.

in the head Bay and along the Bangladesh coast may be explained as a result of the eastern boundary of the anticyclonic gyre.

8. Conclusions

The wind induced circulation of the Bay of Bengal has been studied with a vertically integrated numerical model using different open-boundary conditions. Our main conclusions are:

- The modified Orlanski radiation condition (Camerlengo and O'Brien 1980) is the best suited open boundary condition for the model.
- The model realistically simulates the currents with only slight deviations from available climatological/observed features.
- Upwelling and the downwelling zones estimated by the model are in general agreement with available observations and are consistent with the dynamics of currents.
- Although the model is barotropic, it is able to simulate the major features of the circulation including the eddies. The results are in good agreement with those produced by a more computationally expensive model of the Indian Ocean (Potemra *et al* 1991).

References

Anderson D L T and Moore D W 1979 Cross equatorial jets with special relevance to very remote forcing of the Somali Current; *Deep-Sea Res.* **26** 1–22

Bahulayan N and Varadachari V V R 1986 Numerical model of wind driven circulation in the Bay of Bengal; *Indian J. Mar. Sci.* **15** 8–12

Bahulayan N and Unnikrishnan A S 1992 Simulation of barotropic wind-driven circulation in the upper layers of Bay of Bengal and Andaman Sea during the southwest and northeast monsoon season using observed winds; *Proc. Indian Acad. Sci. (Earth Planet. Sci.)* **101** 47–66

Cane Mark A 1980 On the dynamics of equatorial currents, with application to the Indian Ocean; *Deep-Sea* Res. **A27** 525–544

Camerlengo A L and O'Brien J J 1980 Open boundary conditions in rotating fluids; *J. Comput. Phys.* **35** 12–35

Chapman D C 1985 Numerical treatment of cross-shelf open boundaries in a barotropic coastal ocean model; *J. Phys. Oceanogr.* **15** 1060–1075

Cox M D 1970 A mathematical model of the Indian Ocean; *Deep-Sea Res.* **17** 47–75

Cqx M D 1976 Equatorially trapped waves and the generation of the Somali Current; *Deep-Sea Res.* **23** 1139–1152

Cox M D 1979 A numerical study of Somali current eddies; *J. Phys. Oceanogr.* **9** 311–326

Cox M D 1981 A numerical study of surface cooling processes during summer in the Arabian Sea; In: *Monsoon dynamics* (eds) Lighthill and Pearce, (London, New York, New Rochella, Melbourne, Sydney: Cambridge University Press) pp. 529–540

Das P K, Dube S K and Rao G S 1987 A steady state model of the Somali Current; *Proc. Indian Acad. Sci.* **96** 279–290

Dube S K, Rao A D and Rao G S 1988 Wind induced circulation of the Bay of Bengal; In: *Computational methods in flow analysis* (eds) H Niki and M Kawahara, (Okayama: Univ. of Science Press) vol. 2 pp. 1278–1284

Dube S K, Luther M E and O'Brien J J 1990 Relationship between the interannual variability of ocean fields and the wind stress curl over the Arabian Sea and the Indian summer monsoon rainfall; *J. Meteorol. Atmos. Phys.* **44** 153–165

Düing W 1970 *The monsoon region of the currents in the Indian ocean* (Honolulu: East West Centre Press) pp. 68

Gent P R, O'Neill K and Cane M A 1983 A model of the semiannual oscillation in the equatorial Indian Ocean; *J. Phys. Oceanogr.* **13** 2148–2160

Heaps N S 19 3 Three-dimensional model of the Irish Sea; *Geophys. J. R. Astron. Soc.* **35** 99–120

Hurlburt H E and Thompson J D 1976 A numerical model of Somali Current; *J. Phys. Oceanogr.* **6** 646–664

Johns B, Dube S K, Mohanty U C and Sinha P C 1981 Numerical simulation of the surge generated by the 1977 Andhra Cyclone; *Q. J. R. Meteorol. Soc.* **107** 919–934

La Violette P E 1967 *Temperature, salinity and density of the world's seas* Bay of Bengal and Arabian Sea Informal Rep. of Naval Oceanographic off. (Washington DC, USA), pp. 89

Legeckis R 1987 Satellite observations of western boundary currents in the Bay of Bengal; *J. Geophys. Res.* **92** 12974–12978

Lin L B and Hurlburt H E 1981 Maximum simplification of non-linear Somali Current dynamics; In: *Monsoon dynamics* (eds) Lighthill and Pearce, (London, New York, New Rochella Melbourne, Sydney: Cambridge Univ. Press) pp. 541–555

Luther M E and O'Brien J J 1985 A model of the seasonal circulation in the Arabian Sea forced by observed winds; *Prog. Oceanogr.* **14** 353–385

Luther M E, O'Brien J J and Meng A H 1985 Morphology of the Somali current system during the south-west monsoon; In *Coupled ocean-atmospheric models* (ed) J C J Nihoul (Amsterdam: Elsevier) pp. 405–437

McCreary J P and Kundu P K 1985 Western boundary circulation driven by an alongshore wind: With application to the Somali Current System; *J. Mar. Res.* **43** 493–516

McCreary J P and Kundu P K 1988 A numerical investigation of the Somali Current during the south-west monsoon; *J. Mar. Res.* **46** 25–28

Molinari R L, Olson D and Reverdin G 1990 Surface current distribution in the tropical Indian Ocean derived from compilations of surface buoy trajectories; *J. Geophys. Res.* **95** 7217–7238

Nihoul J C J 1975 *Modelling of marine systems*; (Elsevier Scientific publication Co.) pp. 272

Philander S G H and Delacluse P 1983 Coastal currents in low latitudes (with application to the Somali and El Nino Currents); *Deep-Sea Res.* **30** 887–902

Potemra J T, Luther M E and O'Brien J J 1991 The seasonal circulation of the upper ocean in the Bay of Bengal; *J. Geophys. Res.* **96** 12667–12683

Rao D P 1977 A comparative study of some physical processes governing the potential productivity of the Bay of Bengal and Arabian Sea; Ph. D. thesis, (Waltair: Andhra Univ.) pp. 135

Simmons R S, Luther M E and O'Brien J J 1988 Verification of a numerical ocean model of the Arabian Sea; *J. Geophys. Res. Oceans* **93** 15437–15453

Somayajulu Y K, Ramana Murty T V, Prasanna Kumar S and Sastry J S 1987 Hydrographic characteristics of central Bay of Bengal waters during southwest monsoon of 1983; *Indian J. Mar. Sci.* **16** 207–217.